MATHEMATICAL THEORY OF MULTICOMPONENT DIFFUSION

THE MATHEMATICAL THEORY OF MULTICOMPONENT DIFFUSION WITH APPLICATION TO TRANSFORMATIONS IN THE IRON-RICH ALLOYS OF IRON-MANGANESE-CARBON

By

DIETER WEICHERT, B.A.Sc.

A Thesis
Submitted to the Faculty of Graduate Studies
in Partial Fulfilment of the Requirements
for the Degree
Master of Science

McMaster University
May 1963

MILLS MEMORIAL
LIBRARY
McMASTER UNIVERSITY

MASTER OF SCIENCE (1963)
(Physics)

McMASTER UNIVERSITY
Hamilton, Ontario

TITLE: The Mathematical Theory of Multicomponent Diffusion with Application to Transformations in the Iron-Rich Alloys of Iron-Manganese-Carbon

AUTHOR: Dieter Weichert, B.A.Sc. (University of British Columbia)

SUPERVISOR: Professor J. S. Kirkaldy

NUMBER OF PAGES: v, 44

SCOPE AND CONTENTS:

A theoretical study reducing the general diffusion solution in a multicomponent system to an eigenvalue problem is carried out. Certain properties of the diffusion coefficient matrix are investigated. Special solutions are obtained for a ternary finite diffusion couple and for a moving phase boundary in an infinite medium involving diffusion on both sides of the interface. The latter solution is used to study the kinetics of the growth of proeutectoid ferrite in ternary Fe-Mn-C austenite. Information on the iron-rich corner of the ternary Fe-Mn-C phase diagram in the temperature range from 725°C to 790°C has been obtained experimentally, and the diffusion coefficient of manganese in α-iron has been determined.

ACKNOWLEDGEMENTS

The author is indebted to his supervisor, Dr. J. S. Kirkaldy, for suggesting the problems treated here, and for his advice and encouragement during the course of this work.

Thanks are due to the post-doctoral fellows, Drs. L. C. Brown, J. E. Lane and G. R. Purdy of the Metallurgy Department of McMaster University, Hamilton, Canada, for many stimulating discussions, and to Mr. R. J. Brigham, graduate student in the same department, for inspiring the problem treated in Section Ic.

The financial assistance of the National Woodrow Wilson Fellowship Foundation and the International Nickel Company is gratefully acknowledged.

TABLE OF CONTENTS

LIST OF TABLES[*]

LIST OF ILLUSTRATIONS[*]

---

[*] Tables and illustrations have been placed at the end of the thesis.

INTRODUCTION

Diffusion is the transport of material due to the random thermal motions of the material particles. In analogy to Fourier's Law for heat conduction Fick[1] in 1855 wrote a linear relationship between the flux, J, of a substance and its density gradient, ∇C,

$$J = -D\nabla C \tag{1}$$

This expression is generally known as Fick's first law, but, since there is neither an a priori reason for assuming a linear relation between the flux and the gradient, nor to call D a constant, (1) is merely a definition of the diffusion coefficient, D. However, in many cases of practical interest the concentration gradients occurring are small, so that higher order terms in the gradient can be neglected, and in the concentration range used, D can often be usefully approximated by an average constant value. If (1) is combined with the differential form of the continuity equation for the substance under consideration, one obtains the differential equation of diffusion,

$$\frac{\partial C}{\partial t} - \nabla\cdot(D\nabla C) = 0 \tag{2}$$

In 1945 Onsager[2] generalized Fick's first law to the simultaneous diffusion of several components by writing the flux of the i-th component as a linear combination of all gradients in the system

$$J_i = -D'_{ik}\,\nabla C_k \quad * \tag{3}$$

---

* The summation convention over doubly appearing indices is used throughout this thesis. Subscripts carrying a prime are summed over the range 1 to r-1, while the summation otherwise extends to r, the number of components of the system. In sections where no differentiation between the ranges of summation is required, the primes are omitted.

An alternative phenomenological description has been suggested by Onsager and Fuoss[3],

(4) $$J_i = -L_{ik}\nabla\mu_k ,$$

where the μ_k are the chemical potentials of the components. Although this is more fundamental, since the forces for diffusion are represented as free energy gradients, the description in terms of concentrations is chosen for most diffusion problems.

It will usually be possible to eliminate one of the fluxes by an appropriate choice of coordinate axes. If the concentrations are expressed in moles per unit volume and if local equilibrium exists so that we can write $$C_r = C_r(C_1,\ldots C_{r-1})$$

equations (3) can be re-written as

(3.a) $$J_i = - D_{ik'} \nabla C_{k'} \qquad (i, = 1,\ldots r-1),$$

where $$D_{ik} = D'_{ik} + \frac{\partial C_r}{\partial C_k} D'_{ir}$$

The generalized diffusion equation becomes then

(5) $$\frac{\partial C_i}{\partial t} - \nabla\cdot(D_{ik'} \nabla C_{k'}) = 0$$

where the D_{ik} is now a square matrix of order r-1 for an r-component system.

Solutions of (2) are well known in mathematical physics, while interest in multicomponent diffusion has only comparatively recently resulted in solutions for (5), of which particularly the work of Gosting and Fujita[4] for liquid electrolytes and of Darken[5] and Kirkaldy[6-10], who worked with metallic alloys, is to be noted. However, for more than three components the mathematical and analytical difficulties become rather prohibitive, and no work seems to have been done in systems of higher order than ternary.

Whenever two phases of different composition coexist in a metallic alloy, the growth of one phase into the other will involve a transfer of one or more components across the interface. If the growth follows a parabolic rate law, i.e. if $x/t^{1/2}$ is constant, where x is the distance of advance and t the corresponding time, one accepts this as strong evidence that the growth is diffusion controlled and that local equilibrium obtains at all interfaces. The case of moving boundaries in binary systems has been treated by Danckwerts[11], and solutions for ternary systems were given by Kirkaldy[8].

The principle of local equilibrium may be stated as follows: "For most irreversible processes involving moderate gradients, it will generally be true that the change in an intensive variable within one mean free path will be negligible compared with the magnitude of the variable at that point". When the above is applied to a phase transformation, in particular to the volume element containing the moving interface, the concentrations on both sides of the planar interface can be specified as the equilibrium concentrations given by the isothermal phase diagram. This diagram is the most convenient representation of the equilibrium conditions between the components of the system. In regions of composition in which two phases coexist, tie-lines connect the equilibrium compositions of these phases. (See Fig. 1)

THEORY

I (a) Multiple Diffusion Solutions as an Eigenvalue Problem

1) Review of existing binary diffusion solutions for constant D

In many cases of practical interest diffusion occurs over a range of concentrations small enough for the assumption of a concentration independent diffusion coefficient to be a justifiable approximation. The binary diffusion equation (2) becomes then

$$(6) \qquad \frac{\partial C}{\partial t} = D\nabla^2 C$$

while (5) reads

$$(7) \qquad \frac{\partial C_i}{\partial t} = D_{ik}\,\nabla^2 C_k$$

Solutions to (6) are obtained in three fundamentally different ways. Boltzmann[13] showed that the substitution $\lambda = x/t^{1/2}$ reduced the one-dimensional form of (6) to an ordinary differential equation. A solution is then easily obtained as an integral over the Gaussian function

$$(8) \qquad C(\lambda) = C_o + C_1 \int e^{-\lambda^2/4D} d\lambda \quad ; \quad \lambda = x/t^{1/2}$$

where C_o and C_1 are constants. This solution is stationary in λ-space, which property makes it particularly useful in describing diffusion with moving boundaries. Because of the linearity of (6) any given boundary conditions can be fitted by a superposition involving a finite or infinite number of solutions of the type (8).

The occurrence of the Gaussian in (8) suggests the following solution in x-space:

$$(9) \qquad C(x,t) = C_o + C_1 (4\pi Dt)^{-1/2}\, e^{-(x-\xi)^2/4Dt}$$

That (9) satisfies (6) is easily seen by direct substitution. Since

$$\lim_{t\to 0} (4\pi Dt)^{-1/2} e^{-(x-\xi)^2/4Dt} = \delta(x-\xi) = \infty \; ; \; x = \xi$$

$$= 0 \; ; \; x \neq \xi$$

and $$\int_{-\infty}^{+\infty} \delta(x-\xi)\, d\xi = 1$$

is one of the definitions of the functional $\delta(x)$, (9) obviously describes the space-time behaviour of an amount C_1 of the diffusing substance, which occupies the position $x = \xi$ at time zero. Indeed, one could have guessed (9) from the notion that random movements of the particles (atoms) are responsible for diffusion. The assumption of a constant diffusion coefficient shows its physical meaning clearly at this point: it merely says that every Gaussian distribution of form (9) will spread independently of other such functions in its neighbourhood. Therefore, the solution for any initial concentration can be built up by superposition. Thus, if

$$C(x,0) = c(x)$$

$$C(x,t) = (4\pi Dt)^{-1/2} \int_{-\infty}^{+\infty} c(\xi)\, e^{-(x-\xi)^2/4Dt}\, d\xi \tag{10}$$

This superposition leads to the well-known error function and related solutions, if C(x,0) is of simple analytic form, e.g. if it is constant over finite intervals.

If one assumes the existence of a solution to (6) of the form

$$C(x,t) = c_1(x)\, c_2(t) \quad , \tag{11}$$

then (6) separates into two ordinary differential equations

(12) $$\frac{d^2c_1}{dx^2} + n^2c_1 = 0$$

and

$$\frac{dc_2}{dDt} + n^2c_2 = 0 \quad , \text{ where n is some constant,}$$

and one obtains the solutions

(13) $$C(x,t) = c_1(x)\, c_2(t) = A_n\, e^{-n^2Dt}\, e^{inx}$$

This solution is again fitted to the initial and boundary conditions by a superposition, which in general will now be a Fourier integral or a Fourier series expansion of $C(x,0)$.

A third method of obtaining solutions for binary diffusion is the use of the Laplace transformation[14]. Its main advantage is that the partial differential equation is changed into an ordinary differential equation in x. Its solution will be the Laplace transform of the time-dependent solution. The latter is then obtained from existing tables of Laplace transformations[14]. Both types of solutions, the error function as well as the trigonometric types, can be obtained in this way. The former is preferable for short times, while the latter becomes useful at later times for finite diffusion ranges.

2) <u>Multicomponent diffusion</u>

To find solutions for multiple diffusion satisfying (7), Kirkaldy[10] has suggested that the combination Dt occurring in all known time dependent solutions of the binary case be replaced by the product $u_k t$ and that the solution for the j-th component, C_j, be written as a linear superposition of functions C^k

(14) $$C_j = a_{jk} C^k \quad ,$$

where the $C^k = C(\underline{r}, u_k t) = C(\underline{r}, L^2)$.

The C^k are assumed to satisfy the modified binary diffusion equation

(15) $$\frac{\partial C^k}{\partial t} = u_k \nabla^2 C^k$$

Substitution of (14) into (7) gives

$$a_{ik}\, \partial C^k/\partial t = D_{ij}\, a_{jk}\, \nabla^2 C^k$$

Because of $\frac{\partial C^k}{\partial t} = u_k \frac{\partial C^k}{\partial L^2}$

and (15) one has

$$\frac{\partial C^k}{\partial L^2} = \nabla^2 C^k$$

and the characteristic equations giving the u_k become

$$a_{ik} u_k = u_k a_{ik} = D_{ij} a_{jk} \qquad (16)$$

Here the u_k are to be understood as a diagonal matrix. If one interprets (16) as an equation between the row vectors of the a-matrix, $\underline{a}_k$, one obtains the usual form of an eigenvalue problem[15]

$$D_{ij}\, \underline{a}_k = u_k\, \underline{a}_k \qquad (16\ a)$$

For a system of r dependent components the eigenvalues u_k are given by the r-1 roots of the polynomial in u

$$\mathrm{Det}(D_{ij} - u\delta_{ij}) = 0 \qquad (17)$$

where δ_{ij} is the Kronecker delta. Corresponding to each distinct eigenvalue an eigenvector, $\underline{a}_k$, can be determined which satisfies (16). For roots of multiplicity m, exactly m linearly independent eigenvectors exist[15]. (cf. also Section Ib and Appendix II). However, any multiple of a vector, $\underline{a}_k$, satisfying (16 a) will satisfy the same equations. Therefore, another r-1 conditions are needed to determine the a-matrix uniquely; these will be found to be one of the boundary or initial conditions on the C_j's.

In the case of parametric solutions of type (8), a trial solution similar to (14) can be written,

$$C_j = a_{jk} C^k(\lambda, u_k) \qquad (18)$$

where C^k must now satisfy

$$-\frac{\lambda}{2} \frac{dC^k}{d\lambda} = u_k \frac{d^2 C^k}{d\lambda^2} \qquad (19)$$

for diffusion along one direction. This leads to precisely the same eigenvalue problem as (16). Therefore (18) is also a solution for (7).

The replacement of D by u_k in known solutions of the binary diffusion equation and a linear superposition of all functions, C^k, thus formed, is therefore a generally valid procedure to obtain solutions for the multicomponent diffusion equations with constant diffusion coefficients.

I (b) Properties of the Diffusion Matrix

The time dependence of the solutions of the binary diffusion equation were found to be of the form $\exp(-x^2/4Dt)$ and $\exp(-n^2Dt)$. Clearly, if trial solutions C^k were formed by a substitution of negative eigenvalues for D, these solutions would diverge with time. Similar difficulties arise with the parametric solution in λ-space. The diffusion matrix therefore deserves a closer scrutiny.

In the simplest case of a ternary system Kirkaldy[7] has stated the conditions for physically significant solutions. In a general notation these are[*]

(20.a,b) $\mathrm{Tr}^2(D) \geq 4\mathrm{Det}(D) > 0$

To satisfy the first inequality it is sufficient, but not necessary, for the off-diagonal diffusion coefficients to have the same sign. This does not seem to be true in general, although in the few cases in which interaction coefficients of opposite sign have been measured, one of them could have been equal to zero within the experimental error[16]. While the first inequality (20.a) prevents complex eigenvalues, the condition (20.b) guarantees their positiveness.

In 1962, Haq[17] subjected the condition (20.b) to a detailed investigation. He begins with the usual[7] approximation for the molar fluxes in substitutional alloys

(21) $\sum_i J_i = 0$

This means that lattice sites are conserved, and the effect of vacancies is neglected. It can then be shown[18] that the following relation exists between the coefficients of the phenomenological L-matrix (cf. equ. 4):

---

[*] Tr(D) is the sum of the diagonal elements of D (trace or spur)

(22) $$\sum_{k} L_{ik} = 0$$

To obtain a more fundamental expression for the D-matrix, one[7] now compares equations (4) and (3.a)

(23) $$-J_i = D_{ik'}\,\mathrm{grad}C_{k'} = L_{ij}\mathrm{grad}\mu_j = L_{ij}\mu_{jk'}\,\mathrm{grad}\,C_{k'}$$

where $\mu_{kj} = \frac{\partial\mu_k}{\partial C_j}$. Equating coefficients gives

(24) $$D_{ik} = L_{ij}\mu_{jk}$$

The term $L_{ir}\mu_{rj}$ is eliminated using (22) and the Gibbs-Duhem relations

(25) $$n_i d\mu_i = 0$$

Thus one arrives at*

(26) $$D_{ik} = \frac{1}{n_r} L_{ij'}\,(n_{\ell'} + n_r\delta_{j'\ell'})\mu_{\ell'k}\ .$$

Haq now expresses the concentration C_j by the mole fraction of the components and arrives at

(27) $$D_{ik} = n^2/n_r\, L_{ij'}(n_{\ell'}+n_r\delta_{j'\ell'})G_{\ell'q'}(n\delta_{q'k}-n_{q'})^{-1}$$

Here n is the total number of moles per unit volume, and $G_{\ell q}$ is the Hessian matrix of the Gibbs' free energy per unit volume, $\frac{\partial^2 G}{\partial n_\ell \partial n_q}$; it is necessarily positive definite for a stable system[19]. The L-matrix is of order r-1. It can be written in symmetric form and is then positive definite,[18] i.e. its determinant is positive. Haq further asserts that the determinant of the second matrix is positive. For the determinant of the last term he gives an approximate expression, which again is positive. Since Det(D) is the product of these determinants condition (20.b) will hold for ternary dilute systems.

---

* n_ℓ is a matrix with identical rows, viz. $n_1, n_2, \ldots n_{r-1}$. Similarly, the matrix n_q in (27) has identical columns.

The detailed conditions corresponding to (20.a) and (20.b) for positive eigenvalues of higher order systems are numerous and, for $r > 4$ become quite unmanageable. However, the inverse matrix occurring in (27) can be found explicitly. An expansion by diagonal elements[20] gives

(28) $$\mathrm{Det}(n\delta_{jk} - n_j) = n^{r-1} + n^{r-2}\,\mathrm{Tr}(n) = n^{r-2} n_r > 0$$

since $-\mathrm{Tr}(n) = n_{i'}\delta_{i'} = n_i\delta_i - n_r = n - n_r$

A similar expansion can be used to find all minors, leading to

(28.a) $$(n\delta_{jk} - n_u)^{-1} = \frac{1}{n\,n_r}\,(n_r\delta_{jk} + n_k)^t$$

(cf. Appendix I).

This is, except for the constant, the transpose of the second factor, and the diffusion matrix can now be written as

(29) $$(D) = n/n_r^2\,(L)(N)(G)(N)^t$$

with $(N) = (n_r\delta_{jk} + n_k)$. Since L and G are positive definite, G can be written* as gg^t, and one obtains

(30) $$D = n/n_r^2\,(L)(Ng)(Ng)^t \equiv n/n_r^2\,(L)(S)$$

where S is positive definite*. The diffusion matrix will only be symmetric if L and S commute, which generally will not be the case. However, the eigenvalues of a product of two positive definite matrices are positive, as is proven in Appendix II, and therefore, the diffusion matrix, as written by Haq has only positive characteristic roots.

In a system containing one or more interstitially diffusing components, equation (21) must be replaced by

(31) $$a_i J_i = 0\ .$$

---

* A necessary and sufficient condition for a matrix A to be positive definite is that it can be written $A = aa^t$ (cf. Ref. 15).

The a_i will be zero, or nearly so, for interstitial components, and will have a positive[18] value for other components. DeGroot and Mazur[18] have shown that for a symmetric choice of the L-matrix the restriction (31) leads to

(32) $$a_k L_{ik} = 0$$

Using this expression instead of (22) one arrives, instead of (26), at

(33) $$D_{ik} = \frac{1}{a_r C_r} L_{ij'} (a_{j'} C_{\ell'} + a_r C_r \delta_{j'\ell'}) \mu_{\ell' k}$$

If now mole numbers per unit volume, instead of mole fractions, are used as units of concentrations one sees that $\mu_{\ell k} = G_{\ell k}$ which is the same positive definite Hessian matrix as appears in (27). The term in brackets must be investigated. Its eigenvalues are given by the equation

(34) $$\mathrm{Det}(a_j C_\ell + a_r C_r \delta_{j\ell} - u\,\delta_{j\ell}) = 0$$

Using an expansion by diagonal elements (cf. App. I) one obtains

(35) $$(a_r C_r - u)^{r-1} + (a_r C_r - u)^{r-2}\, \mathrm{Tr}(a_j C_\ell) = 0 ,$$

since all minors of the dyad $a_j C_\ell$ of order two or higher are zero. Hence the eigenvalues are

$$u_{1\,\ldots,\,r-2} = a_r C_r > 0 \text{ (root of multiplicity } r-2)$$

and

$$u_{r-1} = a_{j'} C_{j'} + a_r C_r = a_j C_j > 0$$

The rank of the matrix $(C-uI) = (a_j C_\ell + a_r C_r \delta_{j\ell} - u_i \delta_{j\ell})$, $i = 1 \ldots r-2$, is unity, which is a necessary and sufficient condition[21] for C to be similar to a diagonal matrix. It is demonstrated in Appendix II that therefore the diffusion matrix as written in (33) also has positive characteristic roots only.

I (c) An Example of a Ternary Non-parametric Solution

Kirkaldy[8], and Gosting and Fujita[4] have given solutions for ternary diffusion which are expressed as superposition of functions of the parameter $\lambda = x/t^{1/2}$. Kirkaldy has also given an example of a non-parametric solution of a spherical ternary diffusion field about a point source in an infinite matrix[10].

Another extension of a familiar solution of the differential equation (7) to a finite ternary diffusion field will be given here. It was shown in the previous section that the assumption of separability of the solution satisfying (6) in one dimension and Cartesian coordinates leads to the expression

$$C'(x,t) = a_n e^{-\lambda_n^2 Dt} e^{i\lambda_n x} \tag{36}$$

For a diffusion field that is symmetric about the origin one preferably chooses the real part of the oscillatory exponential and writes the binary symmetric solution

$$C(x,t) = a_n e^{-\lambda_n^2 Dt} \cos \lambda_n x \tag{37}$$

The trial solution for the multicomponent diffusion equation (7) becomes now

$$C_k(x,t) = a_{ko} + a_{kjn} e^{-\lambda_n^2 u_j t} \cos \lambda_n x \tag{38}$$

where the a_{kjn} and u_k must satisfy (16).

A particular case of interest, which will serve well to illustrate the general case, is a three-layer diffusion couple (see Fig. 2), with component two initially distributed uniformly throughout all three layers, while component one is initially confined to the center slab, there having a constant concentration C_{10}. If the origin for this one-dimensional problem is chosen to be the center of the central slab, the boundary conditions are:

(39) $$C_1(x,0) = C_{10}; -\xi < x < \xi \qquad C_2(x,0) = C_{20};$$
$$= 0 ;\ |\xi| < |x| < |L| \qquad -L < x < +L$$

The thickness of the central slab is then 2ξ, while the outside layers measure $(L - \xi)$ each. The second boundary condition is simply the requirement of zero flux across the boundaries:

(40) $$J_i(\pm L,t) = 0 = \pm D_{ik}\, a_{kjn}\, e^{-\lambda_n^2 u_j t} \sin\lambda_n L$$

These conditions will be satisfied if

(41) $$\lambda_n = n\pi/L$$

The Uniqueness Theorem[22] for solutions of the diffusion equations then assures the uniqueness of the solutions (38). Using (39) one obtains the a_{ko} by integrating (38) over all x between -L and +L

(42) $$a_{10} = C_{10}\xi/L$$
$$a_{20} = C_{20} \quad .$$

The rows of the a_{kjn} matrices are now the eigenvectors of D_1 and their scale factors are obtained from an expansion of the initial conditions (39) by the usual procedure for finding Fourier coefficients as follows:

(43) $$a_{kjn}\delta_j = 2\,\overline{C_k(x,0)\cos\lambda_n x} \equiv \Delta_{kn},$$

where the bar designates the average over the whole range. Thus*

(44) $$a_{1jn}\delta_j = 2/L \int_0^L C_1(x,0)\cos(n\pi/L\ x)dx = \frac{2\,C_{10}}{\pi n}\sin(n\pi\xi/L)$$
$$\equiv \Delta_{1n}$$
$$a_{2jn}\delta_j = 0 \equiv \Delta_{2n}$$

---

* Note: the sum is still over j

The u_k are given according to (16) by

$$\text{Det}(D - uI) = 0, \qquad \text{or} \tag{45}$$

$$u^2 - u\text{Tr}(D) + \text{Det}(D) = 0\ ,$$

where Tr(D) denotes the trace of the D-matrix. The eigenvectors are then obtained by using the roots of (45) in (16), and their scale factors are determined from (44). The solutions for the a's can be written in matrix form as follows:

$$a_{kjn} = \frac{1}{u_1-u_2}\left[\begin{pmatrix} D_{11}-u_2 & ; & D_{12} \\ D_{21} & ; & D_{22}-u_2 \end{pmatrix}\begin{pmatrix} \Delta_{1n} \\ \Delta_{2n} \end{pmatrix} ; \begin{pmatrix} D_{22}-u_2 & ; & -D_{12} \\ -D_{21} & ; & D_{11}-u_2 \end{pmatrix}\begin{pmatrix} \Delta_{1n} \\ \Delta_{2n} \end{pmatrix}\right] \tag{46}$$

with

$$u_{1,2} = 1/2\ (\text{Tr}(D) \pm (\text{Tr}^2(D) - 4\text{Det}(D))^{1/2}) \tag{46.a}$$

and $\Delta_{1,2n}$ defined by (44). For $\xi = L/2$, i.e. the center layer having double the thickness of the outer ones, the complete solution becomes:

$$C_k = \begin{pmatrix} \frac{C_{10}}{2} \\ C_{20} \end{pmatrix} + \sum_{m=1}^{\infty} \frac{(-)^{m+1} 2C_{10}}{\pi(2m-1)(u_1-u_2)} \begin{pmatrix} D_{11}-u_2 & ; & D_{22}-u_2 \\ D_{21} & ; & -D_{21} \end{pmatrix} \begin{pmatrix} e^{-u_1 t} \\ e^{-u_2 t} \end{pmatrix}^{\lambda_m^2} \cos \lambda_m x \tag{47}$$

where now $\lambda_m = \frac{(2m-1)\pi}{L}$. If u_1 should equal u_2 the solutions break down; however, a limiting solution can easily be obtained by L'Hospital's rule. An example of such a solution is given by Kirkaldy[7].

The solutions (47) could be useful for a measurement of the interaction coefficient D_{21}. To demonstrate a special case it will be assumed that $D_{21}D_{12} \ll D_{11}D_{22}$, while D_{11} and D_{22} are approximately the same. Then (46.a) reduce to

(47.a) $\quad u_{1,2} \doteq D_{11} \doteq D_{22} \doteq D$ and the solutions become

$$C_1 = a_{10} + \sum_{m=1}^{\infty} \frac{2C_{10}(-)^{m+1}}{\pi(2m-1)} e^{-D\lambda_m^2 t} \cos \lambda_m x \tag{47.b}$$

(47.b) $$C_2 = a_{20} + \frac{2C_{10}(-)^m}{\pi(2m-1)} D_{21}\lambda_m^2 t\, e^{-D\lambda_m^2 t} \cos \lambda_m x$$

The amplitude of the Fourier components of C_1 decay from the beginning, the second term being one third of the first at time zero; after a time $D\lambda_1^2 t=1$, the concentration of component one is given by the first cosine term of (47.a) with an accuracy of about one part in ten thousand. The temporal behaviour of (47.b) is less simple. At very short times the contribution of the terms with high m is large. They will add to give the initially uniform concentration C_2 a small kink at $x = \pm\xi$. However, the terms of high order will soon reach their maximum amplitude at a time $tD\lambda_m^2 = 1$, and then decay rapidly. Thus, when the first cosine term in (47.b) reaches its peak, the second one has decayed to ca. 0.1% of the former, and both solutions C_1 and C_2 can well be approximated by one cosine term. The solutions for the time $t = L^2/\pi^2 D$ are thus (cf. Fig. 2):

(47.c) $$C_1 = \frac{C_{10}}{2} + \frac{2C_{10}}{e\pi} \cos \frac{\pi}{L} x$$

(47.d) $$C_2 = C_{20} - \frac{2C_{10}}{e\pi} \frac{D_{21}}{D} \cos \frac{\pi}{L} x$$

I(d) The Complete Solution for a Moving Interface in an Infinite Medium

In the part of this thesis dealing with the experimental determination of transformation rates of supersaturated face-centered (γ-)iron into body centered cubic (α-)iron (Sect. II.b) a diffusion couple is described which consists of an Fe-Mn-C alloy initially present in the γ-phase and an electrolytically pure layer of α-iron. If held at temperatures below the equilibrium point of the α+γ and γ phases, the austenite matrix decomposes into α and γ iron of compositions given by a tie-line in the constitutional diagram, as shown in Figure 1. At low supersaturations the phase change begins at the interface of the couple, where the electrolytic iron serves as a nucleus. However, if growth occurs, the α-iron formed from the original γ-phase will not be in equilibrium with the electrolytic iron. Diffusion of carbon and manganese into the plated ferrite will therefore occur. To analyse this situation, a ternary diffusion solution for the moving interface, taking into account diffusion of both components in front and behind the interface is required, (cf. Fig. 3).

The concentrations in front of the α:γ boundary are given by Kirkaldy[8], or can be found by fitting a solution of the form (18) with C given by (8) to the particular boundary conditions. If α is the stationary position of the interface in λ-space, the boundary conditions are

(48) $$C_i = C_{io} \quad \text{at } \lambda = +\infty$$
$$C_i = C_{i1} \quad \text{at } \lambda = \alpha^+$$

and the solutions for the carbon (component 1) and manganese (component 2) concentrations in front of the interface become

(49) $$C_i = a_{io} + a_{ik}\,\mathrm{erfc}(\lambda/4u_k) \ .$$

The u_k and the a_{ik} are given by (16), the latter except for an arbitrary constant. Because of the particular choice of limits for the integral in (8) the a_{io} become the C_i at $\lambda = +\infty$. If one now defines

(50) $$C_{i1} - C_{io} \equiv \Delta_i \ ,$$

The boundary conditions for α^+ lead to

(51) $$\Delta_i = d_{ik}\delta_k \ ,$$

where $d_{ik} = a_{ik}\mathrm{erfc}(\alpha/4u_k)$ has been used.

The equations (51) are formally identical with (44), only the Δ_i have different meaning, and d_{ij} stand for a_{ijn}. The solutions (46) are therefore applicable and read:

$$d_{ij} = \frac{1}{u_1 - u_2} \left[\begin{pmatrix} D_{11}-u_2 \,; & D_{12} \\ D_{21} \,; & D_{22}-u_2 \end{pmatrix} \begin{pmatrix} \Delta_1 \\ \Delta_2 \end{pmatrix} ; \begin{pmatrix} D_{22}-u \,; & -D_{12} \\ -D_{21} \,; & D_{11}-u_2 \end{pmatrix} \begin{pmatrix} \Delta_1 \\ \Delta_2 \end{pmatrix} \right] \tag{52}$$

The eigenvalues of the D-matrix are as before

$$u_{1,2} = 1/2 \; (\mathrm{Tr}(D) \pm (\mathrm{Tr}^2(D) - 4\mathrm{Det}(D) \,)^{1/2}) \tag{52.a}$$

For diffusion opposite to the direction of advance of the interface, solutions can be written similarly to (49)

$$C_i' = C_{io}' + d_{ik}' \; \mathrm{erfc} \; (-\lambda/4u_k')/ \; \mathrm{erfc}(-\alpha/4u_k') \tag{53}$$

where the primes denote quantities referring to backward* diffusion.

The velocity, v, of the growing ferrite face becomes in λ-space

$$v = \alpha/2t^{1/2} \tag{54}$$

where $\lambda = \alpha$ is the stationary position of the face in λ-space. To determine the parameter α, the mass balance equations for all components must be solved simultaneously. Each balance equation contains three unknowns, viz. the concentrations C_j of the j-th component in front and behind the interface, and α. One further relation between the interface concentrations of each component is obtained from the constitutional diagram. Thus the balance equations fully determine α. Conversely, with α known, information about the phase diagram could be obtained.

---

* The term forward will be used to refer to quantities and direction on the austenite side of the interface and the direction of its advance; the term backward for the opposite.

One usually writes* an instantaneous mass balance as follows[8]

$$(55) \qquad -J_i(\alpha) = -(C_{i1} - C'_{i1})v = D_{ik}a_{kj}\ d/dx(\mathrm{erfc}(\lambda/2u_j^{1/2}) \Big|_{\lambda=\alpha}$$

Using (54) this becomes

$$(56) \qquad -(C_{i1} - C'_{i1})\alpha/2 = D_{ik}a_{kj}(d/d\alpha(\mathrm{erfc}(\beta_j))\ ,$$

where $\beta_j = \alpha/2u_j^{1/2}$

A different way of writing the mass balance is to equate the total mass changes before and behind the interface[23]. One then obtains:

$$(57) \qquad (C_{io} - C'_{i1})\alpha = \int_{\alpha}^{\infty}(C_i - C_{io})d\lambda \equiv 2a_{ij}u_j^{1/2}\mathrm{ierfc}(\beta_j)$$

The function ierfc(z) is hereby defined as the integral over erfc(z) from z to infinity.

The place of a simple exponential in the first form of the balance equation (55) is taken by an integral over the complementary error function in the second form, equation (56); however, the latter contains only one matrix, while the former is the product of two 2 by 2 square matrices. Also, tables of the function ierfc(z) exist[24], and therefore the second expression for the mass balances seems generally preferable. The mathematical identity of the two equations can be proven via the indicial equations for the u_k. (cf. Appendix III)

Using the total mass balance in the following one can write, with reference to Figure 3,

Areas (I + II) = Area (III)

Inserting the solutions (49) and (53) one obtains

---

* Diffusion in the forward direction only is written for the purpose of comparison of the instantaneous and total mass balances.

$$2u_j'^{1/2} a_{ij}' \int_{-\infty}^{0} dy \operatorname{erfc}(-y) + 2u_j^{1/2} a_{ij} \int_{\beta_j}^{\infty} dy \operatorname{erfc}(y) = (C_{io}-C_{io}')\alpha - 2u_j'^{1/2} a_{ij}' \int_{0}^{\beta_j'} dy \operatorname{erfc}(-y)$$

Obvious simplifications and the use of ierfc as defined in (57) finally leads to

$$(58) \quad (C_{io} - C_{io}') = \frac{2d_{ij}'}{\operatorname{erfc}(-\beta_j')} + \frac{d_{ij}' \operatorname{ierfc}(\beta_j')}{\beta_j' \operatorname{erfc}(-\beta_j')} + \frac{d_{ij} \operatorname{ierfc}(\beta_j)}{\beta_j \operatorname{erfc}(+\beta_j)}$$

The notable contrast between equation (58) and the solution for diffusion on one side of the moving interface only, as given by Kirkaldy[8], is that the functions of concentration and of α are not separable. Therefore (58) can not be solved graphically; instead, a numerical iteration must be applied.

On first sight one may be tempted to write an approximate mass balance, replacing the error functions by triangles, as Zener[23] has done. However, he obtains the height of these triangles from an estimate of the slope of the concentration function at the interface. This is equivalent to keeping the ratio ierfc/erfc fixed at some first trial value, which later must be adjusted, i.e. it is the first step of an iteration. For small values of α it is an excellent approximation to replace the ratio by $1/\pi^{1/2}$, but for larger values of the argument (from about 3 onward) it approaches $1/2\beta$. (cf. Figure 4)

I (e) Approximate Solution for the Special Case of the Advancing Inter Face in the Fe-Mn-C System

For an application to the Fe-Mn-C system the seeming complexity of the equations (58) can fortunately be reduced to relatively simple equations by the introduction of the known diffusion data and some features of the isothermal section of the phase diagram of this system. It will prove worth while to connect the terms in (58) to specific phenomena in the overall diffusion process. The first term on the left minus the first two terms on the right reduce to the total segregation[*] behind the interface if both coefficients for diffusion into the ferrite go to zero. With these coefficients not being zero, the complementary error functions in the denominator represent the rounding of the edges at the original interface, due to back diffusion. The second set of terms on the right represents the leakage into the ferrite due to the combined effect of both gradients, while the last terms give the amount of both components pushed ahead of the interface on their mutual gradients. It should be kept in mind, however, that this is a very qualitative picture, prompted by the similarity of the last two sets of terms, and that the two sets of back flow terms cannot strictly be separated.

The diffusion coefficients for austenite at 745°C were established as follows:[**]

$$D_{ij} = 10^{-8}\,\mathrm{cm}^2/\mathrm{sec} \quad \begin{vmatrix} 1 & ; & -0.011 \\ 0 & ; & 10^{-4.6} \end{vmatrix} \tag{59}$$

The term for carbon diffusion on its own gradient, D_{11}, was taken from the work of Wells, Batz and Mehl[25] and has been corrected for manganese content. An extrapolation of results of the latter two authors[26] leads to a diffusion coefficient for manganese in austenite of about $10^{-15}\mathrm{cm}^2/$ sec; however, it was recently reported by Kurdiumov[27] that the diffusion coefficient of substitutional elements in austenite is greatly enhanced upon up-quenching. The value for D_{22} in (59) is therefore taken as about

---

[*] The segregation of a compound is the difference in its concentration in the original austenite and the growing phase.

[**] It should be observed that the diagonal terms of the D matrix are independent of the units in which the concentrations are expressed, but this is not true for the off-diagonal terms. D_{12} in (59) must be used with concentrations in weight percent.

the upper permissible limit, since the effect of a larger D should have become conspicuous in recent electron micro analysis work, which was done on couples used in growth measurements of the type described in this paper[28]. D_{21} was estimated to be ca. 10^{-23} cm^2/sec, [29] which is completely negligible; it was therefore set equal to zero. The other cross term, D_{12}, for carbon diffusion on a manganese gradient was measured by Purdy[29].

The D for diffusion into the ferrite are

$$(60) \qquad D' = 10^{-8}\,\mathrm{cm}^2/\mathrm{sec} \begin{vmatrix} 150 & ; & -150 \times 0.011 \\ 0 & ; & 10^{-2.9} \end{vmatrix}$$

D_{11} is taken from a recent paper by R. P. Smith[30], the D'_{12}/D'_{11} ratio has been assumed to be the same as in austenite diffusion. The manganese term is obtained from a best fit of the experimental data (cf. Section III e) its value is irrelevant for the present purpose of simplifying (58).

For the above values of the D-matrices the equations (52.a) reduce to

$$(61) \qquad u_{1,2} = D_{11}\,,\ D_{22} \quad \text{and} \quad u'_{1,2} = D'_{11}\,,\ D'_{22}$$

to a very good approximation. Substitution into (52) then shows that all terms containing d_{21} and d'_{21} in (58) are zero. Next, the terms arising from the leakage of carbon into the ferrite should be dropped, since the solubility of carbon in α-iron is negligible (cf. Fig. 1). It may be argued, though, that despite the small solubility the large diffusion coefficient of carbon will spread the carbon far enough into the ferrite to make the loss significant. However, the large manganese gradient toward the α-phase will combine with the negative interaction coefficient to halt the carbon flow almost completely, and the carbon which does leak out will soon be reflected from the outside of the thin ferrite layer. Thus, the high carbon diffusion coefficient looses its effectiveness. From the mathematical point of view one should, rather than use physical arguments, substitute the D-values into equations (50), (52), (52.a) and (58) and compare the relative sizes of the terms in (58). This procedure has been carried out; as expected, it leads to the omission of the same terms as the physical argument does. However, no account was taken in the derivation of (58) of the finite width of the ferrite layer. This is a very good approximation for manganese diffusion, since the 0.05 to 0.1 mm width of the ferrite becomes comparable to the diffusion length for manganese only at a time, $t = x^2/D$, of ca. 10^6 sec. For carbon this time is only about 100 sec., i.e. the assumption of an infinite medium will not hold for carbon diffusion into α-iron.

The qualitative reasoning for the omission of the carbon back-flow terms is therefore to be preferred as the better one. To facilitate a numerical investigation of (58), and to aid in later computations, the functions

$$\frac{\mathrm{ierfc}(z)}{\mathrm{erfc}(z)} = f(z) \qquad \text{and} \qquad \frac{\mathrm{ierfc}(z)}{\mathrm{erfc}(-z)} = g(z)$$

have been plotted and are reproduced in Figure 4.

The approximate, but greatly simplified, mass balances for the two components are now

$$\begin{aligned} C_{10} &= (\Delta_1 - 0.011\Delta_2)\, f(\beta_1)/\beta_1 \\ C_{20} &= 2C'_{21}/\mathrm{erfc}(-\beta'_2) + C'_{21}\, g(\beta'_2)/\beta'_2 + \Delta_2 f(\beta_2)/\beta_2 \end{aligned} \tag{61.a,b}$$

where $C'_{io} = 0$ has been used.

The first equation says in effect that the carbon segregation is equal to the forward flow of carbon due to the combined effect of its own and the manganese gradients, while (61.b) expresses that the manganese segregation, $C_{20} - C'_{21}$, is achieved by both forward and backward diffusion on its own gradient only.

Equation (61.b) could be re-written in various forms, one of which is particularly convenient for the present case. Because of the relative magnitude of the two manganese diffusion coefficients, the leading term will arise from backward diffusion. It is therefore advantageous to write

$$C'_{21}/C_{20} = F(\beta'_2)\ (1 - \Delta_2/C_{20}\ f(\beta_2)/\beta_2) \tag{62.b}$$

The function F(z) is defined by

$$F(z) = z\ \mathrm{erfc}(-z)/(2z + \mathrm{ierfc}(z))\ ,$$

and is also plotted in Figure 4.

The two equations to be solved simultaneously for α are now (62.b) and

$$d_{11} = C_{10}\beta_1/f(\beta_1) \tag{62.a}$$

It was pointed out before, that in contrast to the equations for α given by Kirkaldy only the second can be separated into two parts containing α, respectively concentrations only, while the first one cannot. The simultaneous solution therefore cannot be obtained by a graphical method.

II EXPERIMENTAL

II(a) Determination of the Phase Diagram of the Fe-Mn-C System

For any quantitative investigation of growth rates, the supersaturation must be known as a function of temperature and composition, i.e. the phase diagram must be known. Data on the binary iron system are found in the literature[31]; a survey of the data for the iron-carbon system was made by Kirkaldy[32], while for the ternary Fe-Mn-C system information is scarce. For the purpose of the present investigation it was therefore decided to determine some intermediate points between the known endpoints of the $\alpha+\gamma:\gamma$ curves, instead of using the phase diagram as suggested by Wells[33].

It is found that ferrite, which has precipitated along the austenite grain boundaries, is quickly redissolved upon heating. It can be assumed that this redissolution takes place at a temperature for which the respective alloy composition lies on the $\alpha+\gamma:\gamma$ phase boundary curve.

To determine this temperature of redissolution, samples were held at ca. 710°C to 730°C, according to composition, for about 15 minutes, then examined metallographically for ferrite content. They were then kept at progressively higher temperatures for 10 minutes, and the ferrite content examined after each heat treatment. The redissolution temperature could be determined to ca. ± 2°C. Temperature measurements and method of heat treatment are described in Section II b.

In the standard method of determining a ternary diagram, which was used by Wells, an alloy is kept at high temperature for a time long enough (ca. 1200°C) so that a complete austenitization is assured. The specimen is then taken to a specific temperature and held there long enough until equilibrium has been reached. Its ferrite content is then used as an indication whether the lower reaction temperature was above the phase boundary. However, as was reported by Kurdiumov[27], the diffusion coefficient of substitutional elements in austenite is greatly enhanced by up-quenching. A much faster approach to equilibrium should therefore be expected if a substitutional alloy is taken from a low temperature bath to a higher temperature. This explains the fast redissolution observed and described above. It seems to make this method of redissolution superior to the standard method.

The alloys used in this determination were the same as the ones used for growth rate measurements described in Section II b. They were prepared in a non-consumable electrode arc furnace under a helium atmosphere. The 100 gram buttons were turned and melted four times. The ingot was then cold rolled to 5 mm thickness, annealed in argon at 1100°C, then rolled into 1 mm sheet. The Fe-Mn alloys were carburized at 950°C in mixtures of constant CO : CO_2 ratio for about 10 hours, a time sufficient to insure homogeneity. The samples were then quenched in silicone oil and analysed for carbon.

II (b) Growth Rate Measurements

A procedure which was developed by Purdy[35] for controlled growth rate measurement in the Fe-Mn-C system was followed with minor modifications. The alloys prepared as described in the preceeding section were hand ground to ca. 0.7 mm thickness, to remove any surface inhomogeneities. The samples were then plated with a layer of approximately 0.05 mm of iron in a standard electroplating bath. This was followed by a thin copper flash in a standard $CuSO_4$ bath, upon which another thin layer of iron was deposited. This treatment was thought to suppress a change in effective composition and structure of the iron plating after multiple heat treatment.

The diffusion heat treatments were carried out at various temperatures within the α+γ region of the phase diagram in lead baths, the temperatures of which were controlled ($\pm$ 1°C) by proportioning controllers and frequently measured during the course of the anneals using chromel-alumel thermocouples, which in turn were compared with an NRC standard couple. One couple was annealed at a time and then quenched in brine.

As expected, the plated iron acted as nucleus for ferrite growth, and a very closely planar interface grew towards the center of the sample. The original interface could be determined by a line-up of pores at several points in every specimen. These pores were probably due to dirt particles deposited on the ground surface before plating. A typical line-up of pores is shown in Figure 5.

The low manganese alloys (1.5%) were not brought directly to their respective diffusion temperatures. Since the diffusion times for these couples were rather short (20 to 200 sec), the time taken for warming-up, which takes the samples through high supersaturations, would have introduced too large an error into the measurements. The samples were therefore austenitized for one-half minute at 825°C in a second lead pot. According to Purdy[35] the average time required for a sample to come to within 2°C of the reaction bath temperature after transferring it from the high temperature bath was nine seconds. This time was subtracted from the total time in the low temperature bath to obtain the isothermal reaction time. The distance of advance of the interface was measured metallographically. Between five and thirty measurements were taken for each couple, using a calibrated filar eyepiece with an oil-immersion objective lens. The approximate magnification was 1400 X. The results of these measurements are given in Table II. Figures 6 and 7 show some representative plots of growth versus square-root of time.

III DISCUSSION AND CALCULATIONS

III (a) The Phase Diagram

In a recent survey article Kirkaldy[32] has collected and appraised known data on the binary iron-carbon system. Using his averaged curves, the end points of the $\alpha:\alpha+\gamma$ and $\alpha+\gamma:\gamma$ phase boundaries in the ternary Fe-Mn-C diagram can be found. The corresponding end points of these curves on the manganese axis can be taken from the work of Troiano and McGuire[31] on the binary iron-manganese system. However, points of these curves in the ternary region of the Fe-Mn-C diagram given by Wells and Mehl[33] do not agree with the intermediate points as determined by the writer by the method of ferrite redissolution. The latter results are not only consistent within themselves, but they also agree with extrapolations to zero growth rates of growth rate curves obtained by Purdy[35] and the writer. As pointed out in Section II a, equilibrium should have been obtained much faster with the method used in this work than with the method used in 1941 by Wells and Mehl. The results of the present redissolution method are therefore used for further calculations and are collected in Table I, together with the extrapolated temperatures of zero growth of Purdy and the writer. The same data are plotted in Figure 1, and the best fitting $\alpha+\gamma:\gamma$ boundary curve for some temperatures between 730°C and 770°C are shown. The $\alpha:\alpha+\gamma$ boundary is of relatively little importance, because of the small solubility of carbon in ferrite. The end points of this curve on the carbon axis is very nearly independent of temperature, while its change on the manganese axis, as given by

Troiano's work, is of some consequence for the temperature dependence of the slope of the tie-lines.

III(b) Growth Measurements

In Figures 6 and 7 some representative plots of growth of the ferrite interface versus the square root of the corresponding time are shown. For short times the plots are linear which can be accepted as strong evidence, that the transformation is diffusion controlled. The convex portion at the high time end is thought to be caused by beginning impingement of the diffusion fields of internally precipitated ferrite and of the advancing interface, thereby slowing down the transformation rate.

III(c) Temperature Dependence of Diffusion Coefficients

The temperature dependence of the diffusion coefficients is of the form

$$D(T) = D_o \, e^{-E/kT} ,$$

which can be approximated by a linear relation over the temperature range considered. The values of E for carbon diffusion are approximately 1.3 eV while the value of E for manganese is rather uncertain, perhaps 2 eV[36]. All calculations in this section will therefore be based on the ratios of the diffusion coefficients. The temperature dependence of these ratios is then neglected, since it will approximately cancel out. The only remaining directly temperature dependent parameter is $\beta = \alpha/2D_{11}^{1/2}$. In order to compare experimental results with calculations, the former were all reduced to β using the temperature dependence of D_{11} as given above, with $E = 1.3\text{eV}$, and $D_{11}^{(745^\circ C)} = 10^{-8}\text{cm}^2/\text{sec}$, giving $\beta = (1 - 0.007(T - 745^\circ C))\, 10^{-8}\, \alpha/2$. The β-values of the experimental growth rates are given in the last column of Table 2. They are also used in Figure 8.

III(d) Calculation of an Equilibrium Tie-line

To complete the proposed phase diagram discussed in Section III a, at least one equilibrium tie-line must be found, from which other neighbouring lines can be obtained approximately, thus making further growth rate calculations possible. The most growth rate data for the system were obtained for the 1.52 % manganese, 0.210 % carbon alloy. Moreover, for this alloy appreciable growth rates without the necessity of manganese segregation are obtainable, therefore the assumption of local equilibrium across the interface does not seem unreasonable. This was one of the reasons why Purdy based his proposition of a stable tie-line for the system on measurements taken with this particular alloy. To calculate a stable tie-line under the present assumption of forward and backward diffusion of manganese, a value of $\beta = 0.12$, averaged over both Purdy's and the writer's results, is substituted into (62 a) and a d_{11} calculated. The same value of β used in (62 b) gives a segregation ratio, C'_{21}/C_{20}, of practically unity, i.e. no segregation. This fixes the termination of the tie-line on the $\alpha{:}\alpha+\gamma$ curve. Equation (62 a) is now drawn directly onto the phase diagram as a line with the slope given by $d_{11}=0=\Delta_1-0.011\Delta_2$, and intercepting the line $C_2 = 1.52\%$ Mn at the point $C_1 = C_{10}(1+\beta_1/f(\beta_1))$. The intercept of this line and the $\alpha+\gamma{:}\gamma$ phase boundary curve for 760°C gives the second end point of the tie-line. At different temperatures this tie-line should remain nearly parallel, since, with the exception of the termination of the $\alpha{:}\alpha+\gamma$ boundary at the manganese axis, only the relative position, rather than the shape of the phase boundaries changes considerably over the small temperature ranges considered. This one calculated tie-line can now be swung over the other portions of the phase diagram in a regular and continuous fashion. The sections of the phase boundary curves below the calculated line were divided in equal ratios. Not much can be said about the tie-lines in the upper region of the phase diagram, since the argument for keeping the slope of the lines independent of temperature fails there.

III(e) Calculation of the Diffusion Coefficient of Manganese in Ferrite

No diffusion data on manganese in ferrite were available; therefore the growth rate at 760°C is used to obtain an estimate. Again , a d_{11} is obtained from the measured growth rate and plotted as before. The intersection of the line with the 760°C phase curve gives the upper end of the tie-line. Using the tie-line net proposed above, the manganese segregation is found; (61 b) is then solved for $F(\beta_2')$; β_2' can then be read from the plot of F(z) in Figure 4. The value thus obtained for D_{22}' is $(\frac{1}{28})^2 D_{11} = 10^{-10.9}$ cm^2/sec which was already cited in (59).

III(f) Calculation of Growth Curves

Making use of the information obtained under (d) and (e) above a complete growth curve of the 1.5%Mn; 0.21%C alloy can now be calculated. A trial value of β for a temperature T is used in (62 a) and d_{11} plotted as before. The intercept of the d_{11}-line with the phase boundary curve for the temperature considered selects a tie-line. Its lower end determines the segregation of manganese. Then (62 b) is solved for $F(\beta_2')$, using the trial value for the correction term in β_2. This yields β_2' from the plot of F(z). A second trial value is obtained from β_2' and the calculation repeated, if desired. The curve thus calculated is reproduced in Figure 8 together with the pertinent experimental results. The rather sudden break at approximately 735°C reflects the very quick flattening of the F(z) function, enhanced by the relation between d_{11} and the manganese segregation ratio as given by the phase diagram. The agreement between the calculated curve and the experimental one is good and can be accepted as strong evidence for the existence of local equilibrium across the interface.

III(g) Calculations for High Manganese Concentrations

If growth rate curves are calculated according to the above outline for alloys whose initial manganese concentrations lie above the endpoint of the $\alpha:\alpha+\gamma$ boundary curve, it will be found that the calculated curves remain invariably below the observed ones (cf. Figure 8). Indeed, for these concentrations equations (62 a) and (62 b) predict a maximum possible growth rate which is exceeded by experimental values. This calls to mind Purdy's[35] postulate of "constrained local equilibrium" across the interface. It must then be assumed that the approximate local equilibrium, which for low manganese concentrations could justifiably be assumed, no longer holds. Equations (62 a) and (b) are still valid, as they were derived from the mass balances, while the relation between the interfacial concentrations previously given by the tie-lines is now lost. The problem becomes then exceedingly complex, and a possible method of approach is pointed out in Appendix IV.

SUMMARY

(1) Solutions for multicomponent diffusion have been written in eigenvalue problem formulation.

(2) It has been established that the general multicomponent diffusion matrix has only positive eigenvalues. The possibility of oscillatory or divergent diffusion solutions is thus excluded.

(3) The mathematical equivalence of the total and the instantaneous mass balances has been demonstrated.

(4) The $\alpha+\gamma:\gamma$ phase boundary of the iron-rich corner of the Fe-Mn-C phase diagram has been determined in the temperature range from 725°C to 770°C.

(5) An equilibrium tie-line for the above phase diagram has been calculated and a tie-line net for the low manganese portion is proposed.

(6) The diffusion coefficient of manganese in α-iron has been determined as $10^{-10.9}$ cm^2/sec.

(7) Transformation rates of Fe-Mn-C ternary austenites have been calculated and have been found to agree with experimental data for low manganese concentrations.

(8) For high manganese concentrations ($\sim 3\%$) the assumption of local equilibrium across the interface does not appear to hold.

APPENDIX I

The Inverse Matrix $(n\delta_{jk} - n_j)^{-1}$

The inverse of a matrix, a_{jk}, is given by the matrix

$$a^{-1}_{jk} = (-)^{/j-k/}(A_{jk})^t/\mathrm{Det}(a_{jk}) \ ,$$

where t designates the transposed matrix and the A_{jk} are the determinants obtained from a_{jk} by deleting the j-th row and the k-th column. For the calculation of $\mathrm{Det}(N^*) = \mathrm{Det}(n\delta_{jk} - n_j)$ and its minors, an expansion by diagonal elements[20] seems most appropriate. If the general matrix a_{jk}, of order r-1, is written as $(x_j\delta_{jk} + b_{jk})$, then this expansion consists of a sum of products of x_j, taken m at a time, each product mutliplied by its complementary minor of order r-1-m in b_{jk}, the sum taken over such products for all values of m from r-1 to zero. Identifying $(n\delta_{jk} - n_j) = (x_j\delta_{jk} + b_{jk})$, one sees that all principal minors of n_j of order two or higher vanish because their rows are identical. $\mathrm{Det}(N^*)$, being of order r-1, therefore reduces to $\mathrm{Det}(n\delta_{jk} - n_j) = n^{r-1} - n^{r-2}\mathrm{Tr}(n_j) = n_r n^{r-2}$, while the diagonal terms in the inverse of N* become

$$N^{*-1}_{jj} = 1/\mathrm{Det}(N^*) \ (n^{r-2} - n^{r-3}(\mathrm{Tr}(n_j') - n_j) = 1/\mathrm{Det}(N^*) \ n^{r-3}(n_r + n_j),$$

since $\mathrm{Tr}(n_{j'}) = n-n_r-n_j$.

By the interchange of /k-j/ - 1 columns the minors giving the off-diagonal terms of A_{jk} can be changed into a form very similar to the original one, but having $-n_k$ in the diagonal position formerly occupied by $n-n_k$. In the general notation, x_k and hence $\prod_j x_j$ is now zero while the second and only non-zero term in A_{jk} becomes $-n_k n^{r-3}$. If the proper sign, $(-)^{/k-j/}$, of the minor, and the $/k-j/-1$ column changes are taken into account one obtains after some rearranging:

$$(n\delta_{jk} - n_j)^{-1} = 1/nn_r\ (n_r\delta_{jk} + n_k)^t \quad .$$

APPENDIX II

Eigenvalues of Certain Matrix Products

The eigenvalues of the generally non-symmetric matrix product AB of the positive definite matrices A and B are given by the secular equation

$$\mathrm{Det}(AB - uI) = 0$$

A necessary and sufficient condition[15] for B to be positive definite is that it can be written $B = b^t b$. Since $\mathrm{Det}(b) \neq 0$, one obtains the equivalent equation

$$\begin{aligned} \mathrm{Det}(b)\mathrm{Det}(Ab^t b - uI)\mathrm{Det}(b^{-1}) &= 0, \quad \text{or} \\ \mathrm{Det}(bAb^t - uI) &= 0 \end{aligned}$$

Applying the above quoted theorem to bAb^t twice one sees that this product is positive definite. Therefore, the eigenvalues of the product of two positive definite matrices are positive.

To obtain a more specialized result for the eigenvalues of the product of the matrix $C = (a_i C_\ell + a_r C_r \delta_{j\ell})$ and positive definite matrices, as occurring in equation (33) the following considerations are needed. (cf. Ref. 15) A real matrix A with dimensions n by n can be considered as giving a certain transformation of n-space with respect to a given set of orthogonal axes. If the matrix is singular, it represents a projection of n-space onto a space of lower dimension. If A has n linearly independent eigenvectors it is a magnification or reflection of n-space along the directions of this (in general triclinic) set of eigenvectors. If A is positive definite it represents a magnification along an orthogonal set of axes. If A has a negative eigenvalue, the eigenvector corresponding to it will be reflected through the origin, i.e. the relative orientation of the axes will change. If a sequence of magnifications is applied to n-space represented by the matrices G, C and L, and neither of these transformations changes the orientation of the respective axes, the total resulting transformation, represented by the matrix product (L)(C)(G), will leave the relative orientation of any n independent vectors invariant. This total transformation can therefore not include any reflections and hence cannot have negative eigenvalues.

The matrix C has precisely the required properties for above argument to hold. Its eigenvalues are given in the text as $u = a_r C_r$ (with multiplicity r-2) and $a_j C_j$ (simple root). According to reference (21), the sufficient condition for C to have r-1 independent eigenvectors is that the matrix (C - uI) have rank r-1-m = 1, where m is the multiplicity of any multiple root. Clearly, the rank of the remaining dyad $a_j n_\ell$ is one, since all minors of order two or higher are zero.

Therefore the product (L)(C)(G) has only positive eigenvalues.

APPENDIX III

The Mathematical Identity of the Instantaneous and the Total Mass Balances

To prove the mathematical equivalence of (56) and (57) one needs the identity

$$\text{(III.1)} \qquad \operatorname{ierfc}(x) = e^{-x^2}/\pi^{1/2} - x \operatorname{erfc}(x) \, ,$$

which is easily obtained by partial integration. The limit

$$\text{(III.2)} \qquad \lim_{x \to \infty} x \operatorname{erfc}(x) = 0 \, ,$$

as is seen from the asymptotic expansion for large x,

$$\text{(III.3)} \qquad x \operatorname{erfc} \doteq x \, \frac{e^{-x^2}}{2x} \left(1 - \frac{1}{2x^2} + \ldots\right) \, .$$

The two equations (56) and (57) can be rewritten as

$$\text{(III.4)} \qquad (C_{io} - C'_{i1}) \, \alpha/2 = D_{ik} a_{kj} \, 1/(u_j \pi)^{1/2} \, e^{-\beta_j^2} - (C_{i1} - C_{io}) \alpha/2$$

$$\text{(III.5)} \qquad (C_{io} - C'_{i1}) \, \alpha/2 = a_{ij} \, (u_j/\pi)^{1/2} \, e^{-\beta_j^2} - a_{ij} (u_j)^{1/2} \beta_j \operatorname{erfc}(\beta_j) .$$

The equality of the first terms follows at once from the indicial equation, (16), while the second terms are equal by the boundary conditions for α^+.

APPENDIX IV

A Possible Approach to Non-Equilibrium Across the Interface

Equations (62.a) and (62.b) can only be solved for β if a relation between the interfacial concentrations of the components is known. The assumption of local equilibrium assigns these concentrations their equilibrium values, but for the particular case of the growing interface this will at best be a good approximation, since there must always be some free energy difference across the interface if the boundary is to migrate. As the experimental results indicate, the approximation may become rather unjustified in some extreme cases. No approximate relation between the interface concentrations can then be written and one equation for the calculation of a growth rate is lost. The system is seemingly free to choose any two interfacial concentrations for its components, i.e. each of the two end-points of the non-equilibrium tie-line can be chosen from an infinity of points. For irreversible processes having such a degree of freedom (or more) the use of variational principles, similar to Hamilton's principle in classical mechanics or Fermat's principle in optics has been suggested[37]. Under certain restrictions it can be shown that the steady state is defined by a minimum in the rate of entropy production[18]. The limitations of this principle have been reviewed by Callen[38]. As a generalization of this principle to nonstationary states the principle of minimum dissipation has been suggested by Onsager[39] and amplified with specific reference to metallurgical transformations by Kirkaldy[40]. His formalism will be used in the following.

The principle states that the variation

$$\text{(IV.1)} \qquad \delta \int_{\text{volume}} (2J_i X_i - L_{ik} X_i X_k)\, dV = 0$$

specifies the integral behaviour of an unconstrained heterogeneous conduction-diffusion-reaction-viscous flow process, subject to the nonholonomic constraint J_i = constant. In the isothermal system under consideration the fluxes are the diffusive currents of the components while the X_i are the corresponding thermodynamic forces, i.e. the negative chemical potential gradients. The L_{ik} are the phenomenological coefficients defined in equation (4). $J_i X_i$ is the entropy production rate[18]. It is easily seen that the Euler-Lagrange equations of (IV.1) reduce to the phenomenological equations, if L_{ij} is assumed to be constant. In most applications they are not constant which is one of the major difficulties, restricting the use of the principle.

To solve the case of non-equilibrium across the interface (IV.1) could be applied to the problem. To simplify matters the extreme case of zero manganese partitioning shall be considered. This will certainly not be the case; instead, the manganese segregation can be anything between zero and its equilibrium value. However, the assumption of partial equilibrium will not help to clarify the approach, but will, on the contrary, introduce further complications. As an additional unjustified assumption, only the dissipation due to forward diffusion is taken into account. The left end of the non-equilibrium tie-line is thus fixed while its termination at the γ-boundary must be determined. The integral in IV.1 is performed approximately, then the variation is taken with respect to the growth rate parameter β. For the values of the diffusion coefficients given in (59) the entropy production due to carbon flow by far exceeds the other terms in the variational integral, which turns out to be:

$$\text{(IV.2)} \qquad \left(\frac{2d_{11}(\beta_m)\mu_{11}\, d_{11}(\beta)\, \mathrm{erfc}(2^{1/2}\beta_f)}{\mathrm{erfc}(\beta_m)\, \mathrm{erfc}(\beta)} - \frac{d_{11}^2(\beta)\mu_{11}\, \mathrm{erfc}(2^{1/2}\beta)}{\mathrm{erfc}(\beta)\, \mathrm{erfc}(\beta)}\right) = 0$$

where the subscript m indicates the terms to be held constant and where $\beta_f = \beta_m$ for a variation $\beta<\beta_m$ and $\beta_f = \beta$ for $\beta>\beta_m$, due to the fact that the product J_iX_i will be non-zero from the discontinuity of either factor with the larger β to infinity. For d_{11} the equation (62.1) can be used. Differentiation leads then to the trivial solution $\beta = 0$, if no terms are retained which were previously neglected. This is a very obvious extremum of the dissipation, but it does not represent an acceptable solution for the problem. It does, however, illustrate the variational approach, and it is thought that a calculation in which higher order terms are carried, and in which not only partial manganese segregation but also chemical processes at the interface, driven by the interfacial chemical potential difference, are taken into account, may lead to a non-trivial solution.

REFERENCES

1. Fick, A.: Pogg. Ann. 94, 59, (1855).
2. Onsager, L.: Ann. N.Y. Acad. Sci. 46, 241 (1945).
3. Onsager, L. and Fuoss, R.M.: J. Phys. Chem. 36, 2689 (1932).
4. Gosting, L.J. and Fujita, H.: J. Am. Chem. Soc. 78, 1099 (1956).
5. Darken, L.S.: "Atom Movements", American Society for Metals (1951).
6. Kirkaldy, J.S.: Can. Journ. Phys. 35, 435, (1957).
7. Kirkaldy, J.S.: Can. Journ. Phys. 36, 899, (1958).
8. Kirkaldy, J.S.: Can. Journ. Phys. 36, 907, (1958).
9. Kirkaldy, J.S.: Can. Journ. Phys. 36, 917, (1958).
10. Kirkaldy, J.S.: Can. Journ. Phys. 37, 30, (1959).
11. Danckwerts, P.V.: Trans. Faraday Soc. 46, 701, (1950).
12. Kirkaldy, J.S.: "AIME Symposium on the Decomposition of Austenite by Diffusional Processes", Interscience (1962).
13. Boltzmann, L.: Ann. Phys. Leibzig, 53, 959 (1894).
14. Doetsch, K.: "Einfuhrung in die Theorie und Anwendung der Laplace Transformation", Birkhauser Verlag, Basel (1958).
15. Murdoch, D.C.: "Linear Algebra for Undergraduates", Wiley (1957).
16. Dunlop, P.J. and Gosting, L.J.: J. Phys. Chem. 63, 86 (1959).
17. Zia-Ul-Haq, A.H.M.: M.Eng. Thesis, McMaster University (1962).
18. DeGroot, S.R. and Mazur, P.: "Non-Equilibrium Thermodynamics", North Holland Publ. Co. (1962).
19. Landau, L.O. and Lifshitz, E.M.: "Statistical Physics", Addison-Wesley (1958).
20. Aitken, A.C.: "Determinants and Matrices", Interscience (1958).
21. Browne, E.T.: "The Theory of Determinants and Matrices", University of North Carolina Press (1958).

22. Sommerfeld, A.: "Lectures on Theoretical Physics", Vol.6, Academic Press (1956).

23. Zener, C.: J. Appl. Science, 20, 950, (1949).

24. Crank, J.: "Mathematics of Diffusion", Oxford (1957).

25. Wells, C., Batz, W. and Mehl, R.F.: Trans. AIME 188, 553 (1950).

26. Batz, W. and Mehl, R.F.: Trans. AIME 144, 315, (1941).

27. Kurdiumov, G.: "Proc. International Conference on Peaceful Uses of Atomic Energy", 15, 81, (1955).

28. Kirkaldy, J.S., and Purdy, G.R.: Unpublished.

29. Kirkaldy, J.S., and Purdy, G.R.: Can. J. Phys. 40, 202 (1962).

30. Smith, R.P.: Trans. AIME 224, 105, (1962).

31. Troiano, A.R., and McGuire, F.T.: Trans. ASM 31, 340 (1943).

32. Kirkaldy, J.S.: "Symposium on the Advances in Ferrous Physical Metallurgy", to be published.

33. Wells, C.: "Metals Handbook", ASM (1948).

35. Purdy, G.R.: Ph.D. Thesis, McMaster University (1962).

36. Smithels, C.J.: "Metals Reference Book, Vol. 2". Butterworth Scientific Publications (1955).

37. Kirkaldy, J.S.: Can. J. Phys. 38, 1343 (1960).

38. Callen, H.B.: "Proc. Int. Symp. Transport Processes in Statistical Mechanics, Brussels, 1956" Prigogine ed., Interscience.

39. Onsager, L.: Ann. N.Y. Acad. Sci., 46, 241, (1945).

40. Kirkaldy, J.S.: Can. J. Phys. 38, 1356 (1960).

Table I: Temperature of Ferrite Dissolution and of Extrapolated Zero Growth Rates

Alloy	Temperature (°C)
3.80 wt% Mn, 0.096 wt% C	770
" 0.155 wt% C	760
" 0.230 wt% C	740
3.16 wt% Mn, 0.159 wt% C	770 *)
" 0.289 wt% C	750 *)P)
1.52 wt% Mn, 0.335 wt% C	770 *)P)
" 0.405 wt% C	760 *)P)
0.455 wt% C	748

Table II: Measured Ferrite Growth Parameters

Alloy		Temperature (°C)	α ($cm^2/sec^{1/2} x10^{-6}$)	β **)
1.52 wt% Mn, 0.210 wt% C		725	23.8 ± 1.3	0.136
"	"	730	17.6 ± 2.6	0.097
"	"	735	11.9 ± 1.5	0.064
"	"	760	6.8 ± 0.6 P)	0.030
"	"	725	18.0 ± 1.0 P)	0.103
"	"	735	10.4 ± 0.5 P)	0.056
3.16 wt% Mn, 0.159 wt% C		750	9.7 ± 1.0	0.047
"	"	760	7.1 ± 1.0	0.032
3.80 wt% Mn, 0.155 wt% C		735	6.4 ± 0.5	0.034
"	"	740	5.3 ± 0.5	0.028
"	"	750	3.0 ± 0.3	0.015

*) Extrapolated Data

**) $\beta = \alpha/2 \, (D_{\parallel}^{745°C})^{1/2} \, (1 - 0.007 \Delta T)$

P) From Purdy[35]

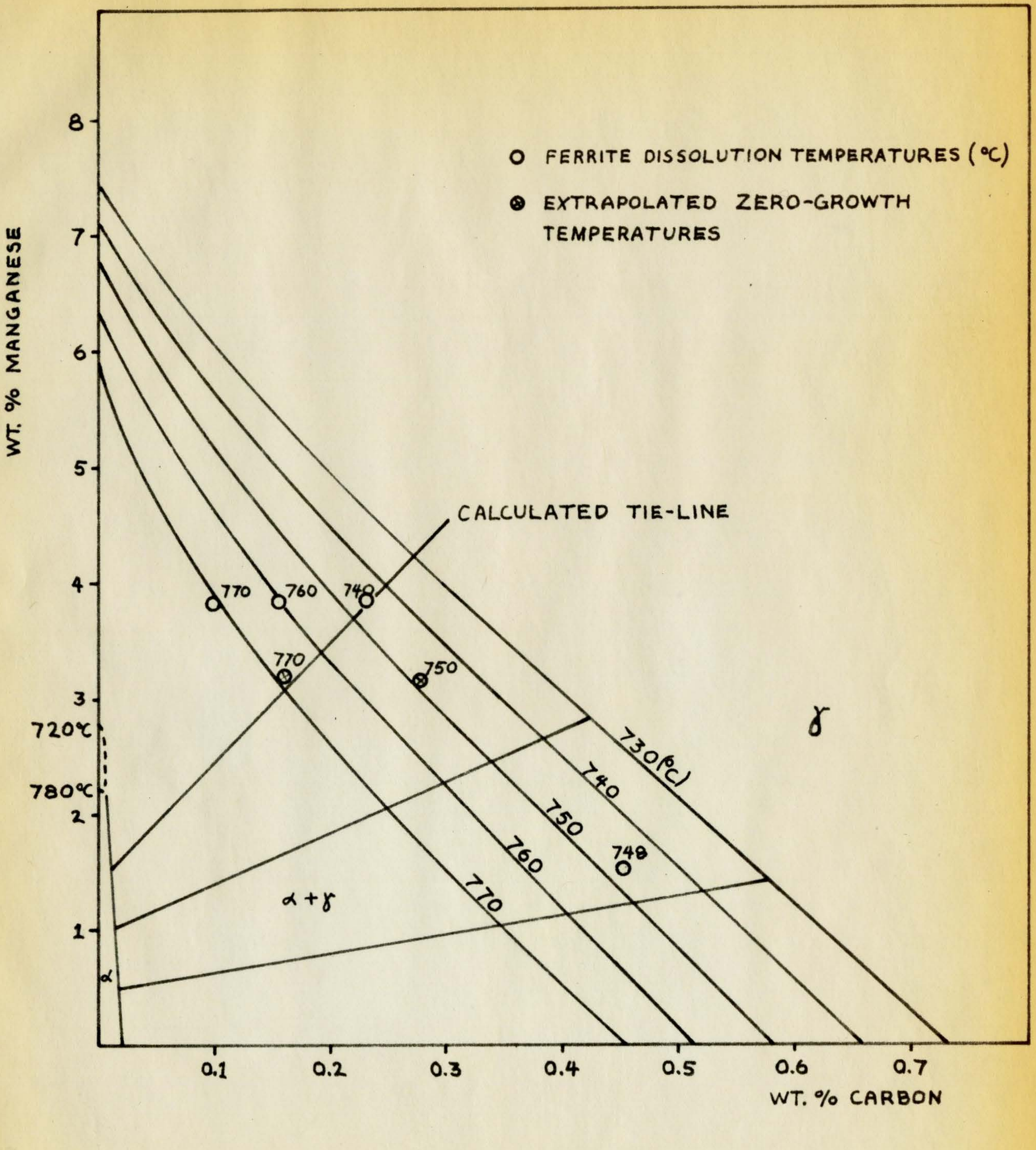

Figure 1. Iron, carbon, manganese constitution diagram, showing equilibrium tie-lines.

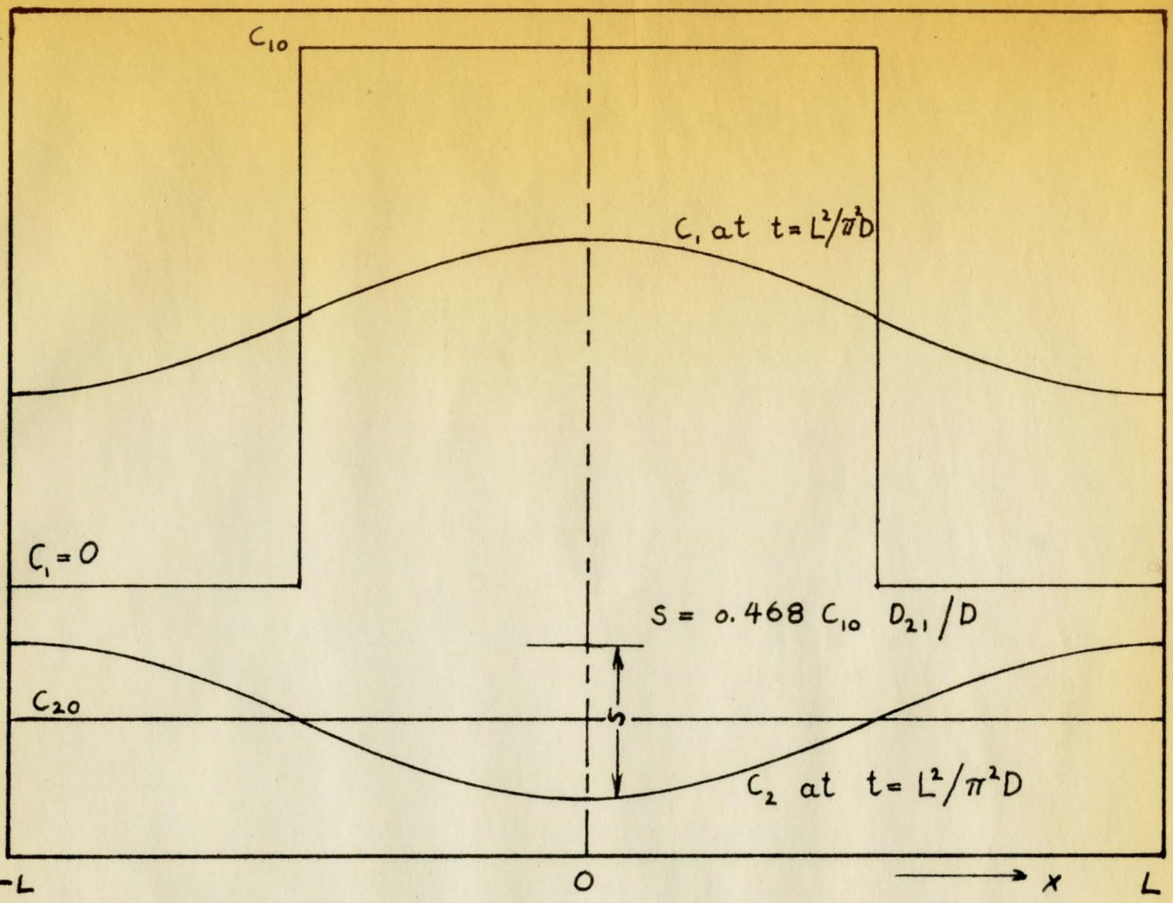

Figure 2. Finite three layer diffusion couple.

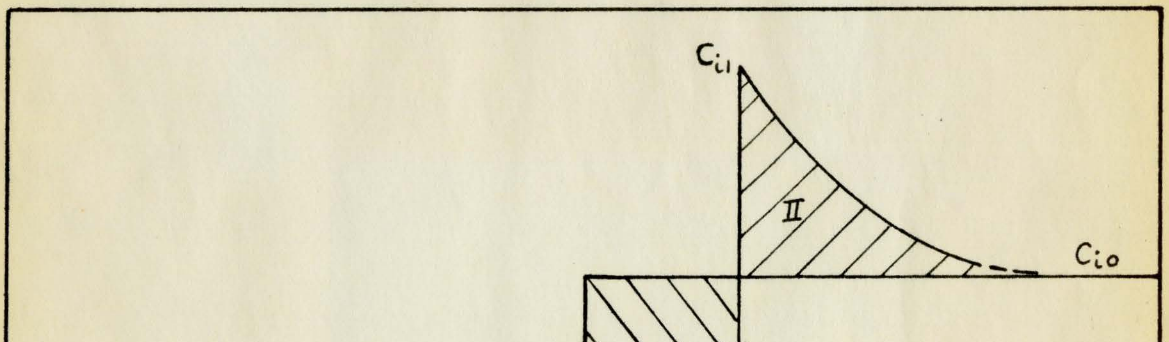

Figure 3. Moving interface in λ-space with forward and backward diffusion.

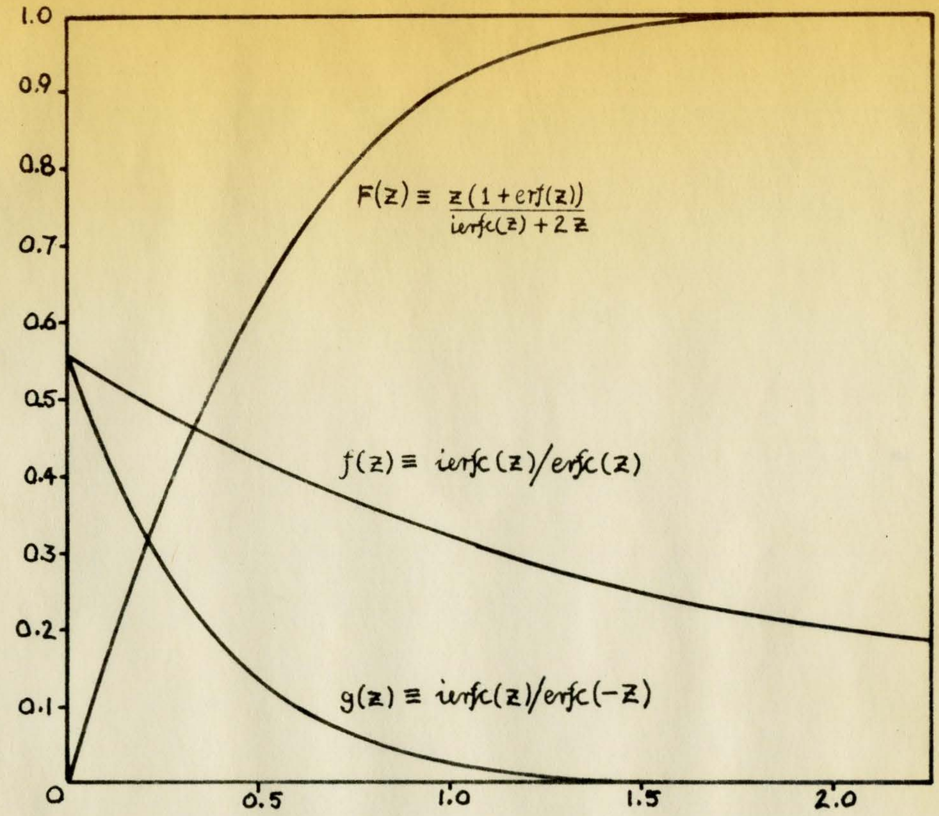

Figure 4. The functions g(z), f(z) and F(z).

Figure 5. A typical diffusion couple, showing pores delineating the original interface (X 2240).

MILLS MEMORIAL LIBRARY McMASTER UNIVERSITY

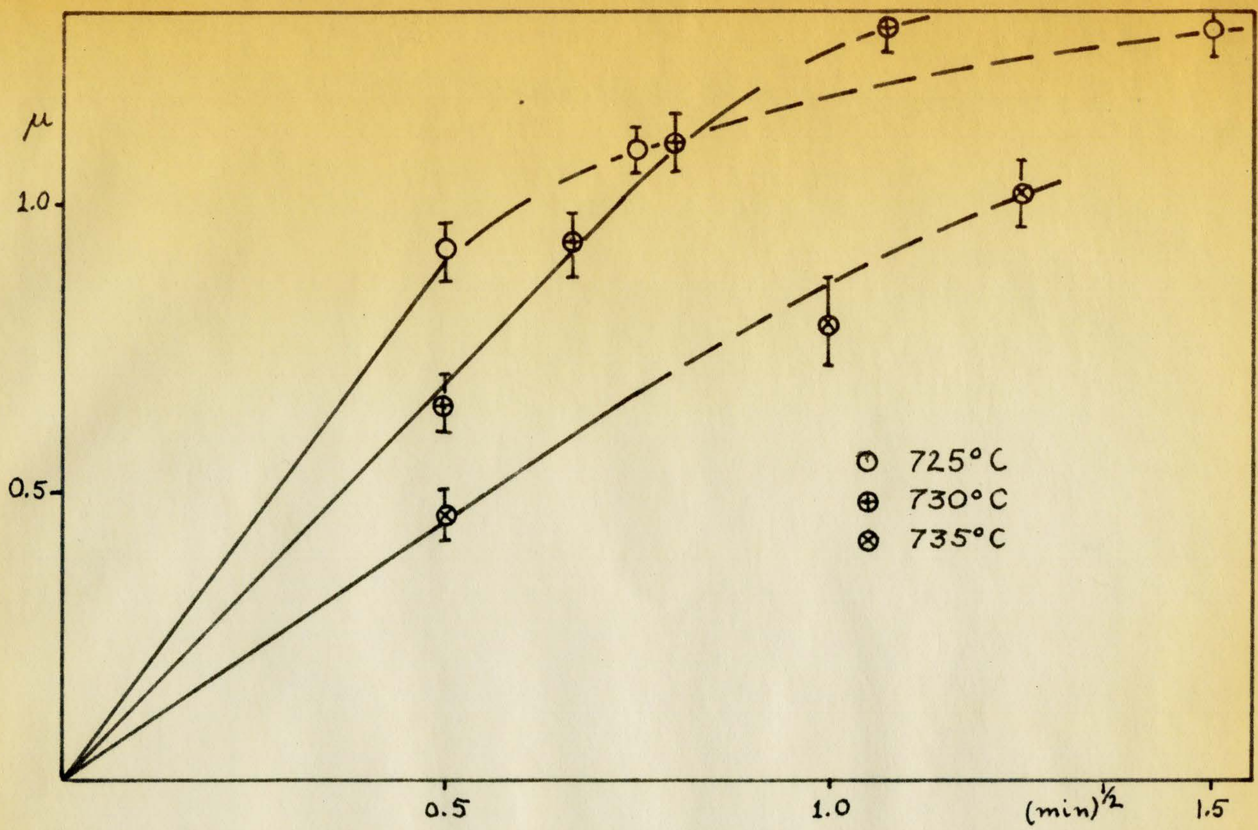

Figure 6. Ferrite growth data for ternary 1.52% Mn, 0.210% C diffusion couples.

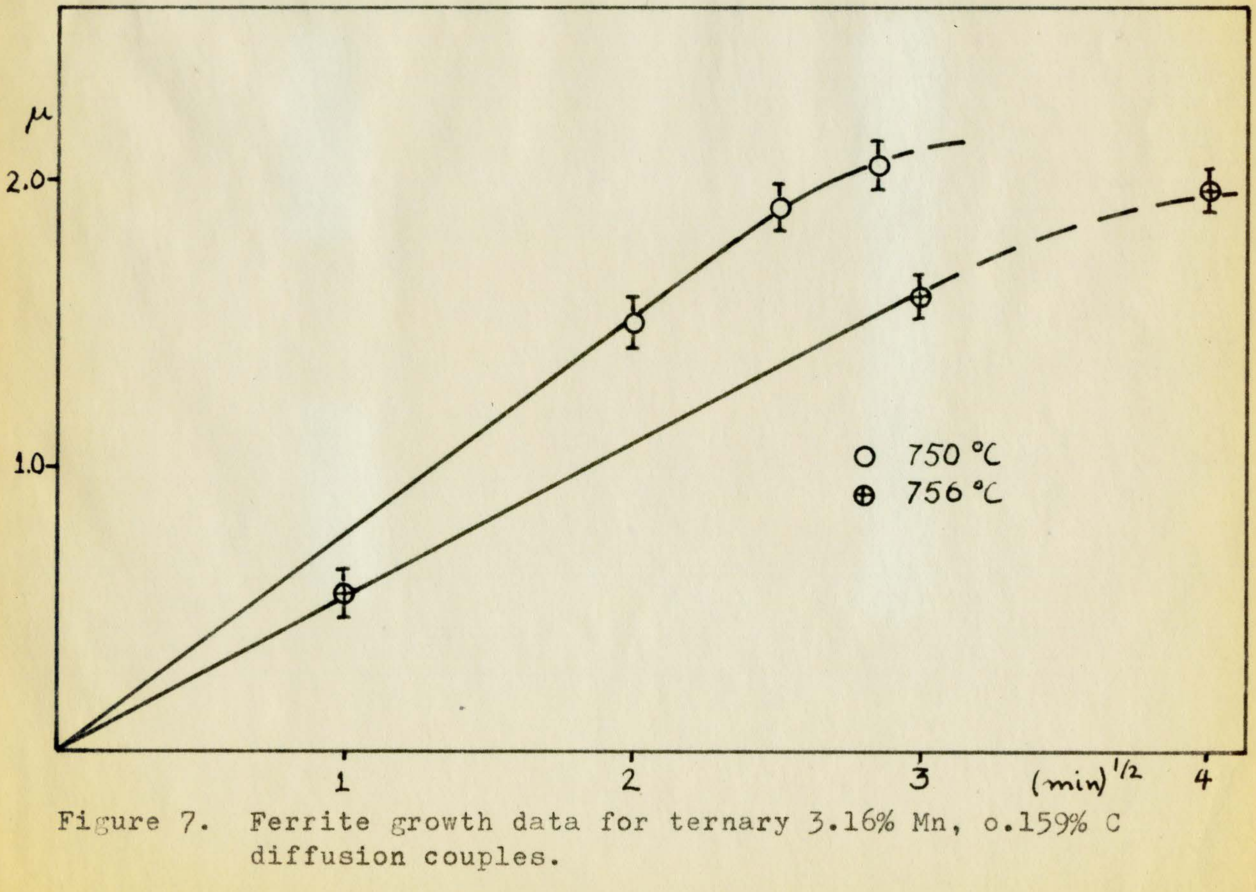

Figure 7. Ferrite growth data for ternary 3.16% Mn, 0.159% C diffusion couples.

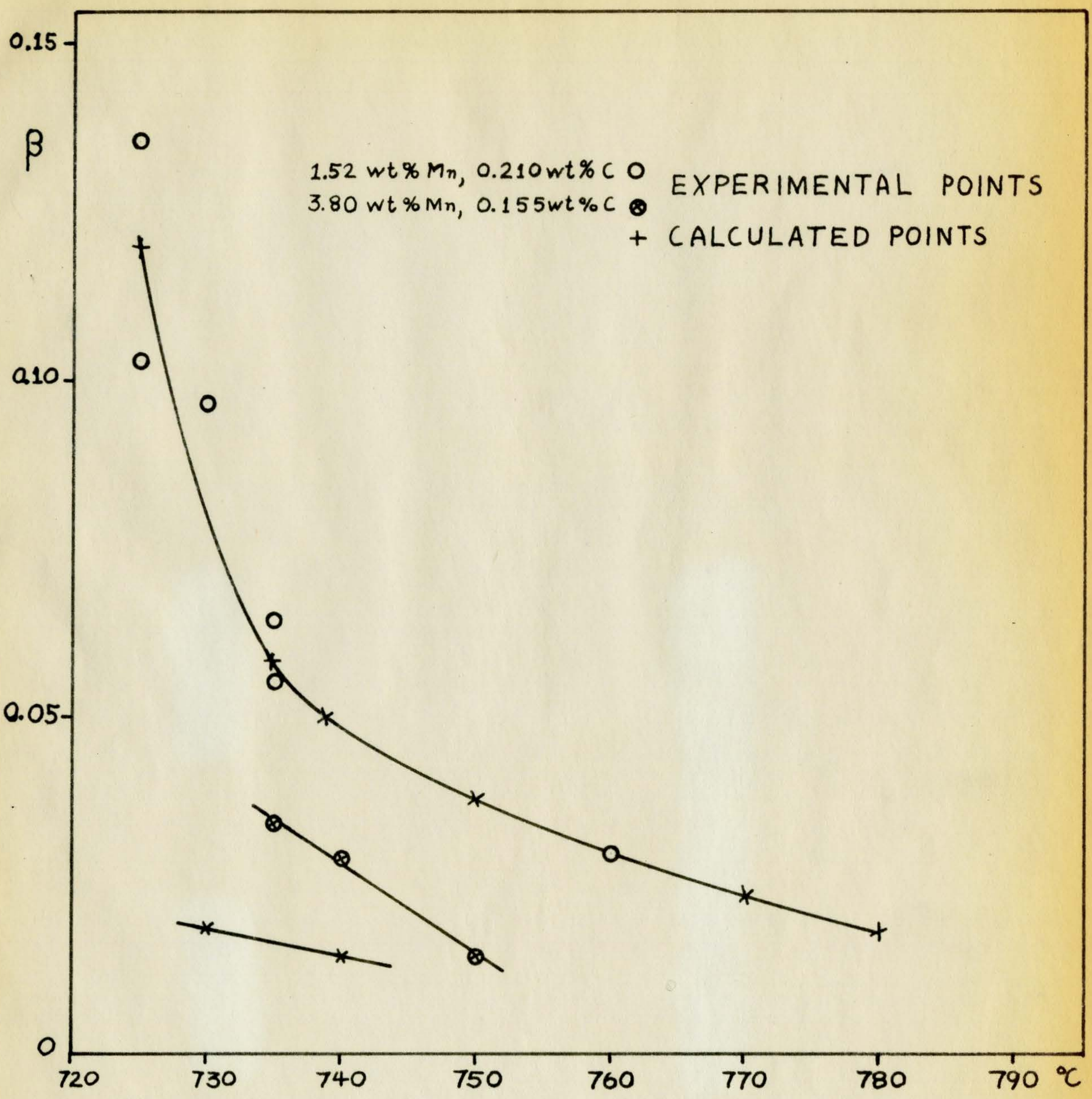

Figure 8. Calculated and experimental growth curves.